Eur. Phys. J. C 51, 875–881 (2007)
DOI 10.1140/epjc/s10052-007-0336-1

THE EUROPEAN PHYSICAL JOURNAL C

Regular Article – Theoretical Physics

Flavor symmetry breaking and scaling for improved staggered actions in quenched QCD

M. Cheng[1,a], N. Christ[1], C. Jung[2], F. Karsch[2], R. Mawhinney[1], P. Petreczky[2,3], K. Petrov[4]

[1] Physics Department, Columbia University, New York, NY 10027, USA
[2] Physics Department, Brookhaven National Laboratory, Upton, NY 11973, USA
[3] RIKEN-BNL Research Center, Brookhaven National Laboratory, Upton, NY 11973, USA
[4] Niels Bohr Institute, University of Copenhagen, Blegdamsvej 17, 2100 Copenhagen, Denmark

Received: 17 April 2007 /
Published online: 27 June 2007 –

Abstract. We present a study of the flavor symmetry breaking in the pion spectrum for the p4-improved fermion action. Three different variants of the p4 action – p4fat3, p4fat7, and p4fat7tad – are compared to the Asqtad and naive staggered actions. To study the pattern of symmetry breaking, we measure all 15 pion masses in the four-flavor staggered theory. The measurements are done on a quenched gauge background, generated using a one-loop improved Symanzik action with $\beta = 10/g^2 = 7.40$, 7.75, and 8.00, corresponding to lattice spacings of approximately $a = 0.31$ fm, 0.21 fm, and 0.14 fm.

PACS. 11.15.Ha; 11.30.Rd; 12.38.Aw; 12.38.-t; 12.38.Gc

1 Introduction

Staggered fermions are widely used to study QCD thermodynamics. They are relatively inexpensive computationally, allowing for the generation of a large ensemble of gauge configurations at several values of the gauge coupling necessary to study thermodynamic observables. Also, the staggered fermion formulation naturally allows for $\mathcal{O}(a^2)$ improvement, which is crucial for calculations of energy density and pressure [1] at lattice spacings corresponding to temporal extents $N_\tau = 4$, 6 and 8 feasible with today's computer technology.

Staggered fermions have only a residual U(1) chiral symmetry, but no flavor symmetry. As a consequence of this only one of the pions becomes massless in the limit of vanishing quark mass. The other pions have masses of $\mathcal{O}(g^2a^2)$ at finite lattice spacing a. As the continuum is approached the complete symmetry group gets restored. In terms of the Symanzik effective theory, violation of flavor symmetry appears as an $\mathcal{O}(g^2a^2)$ effect. It was noticed a long time ago that using smeared links, consisting of nearest-neighbor links and multi-link staples, can reduce the flavor violating effects [2, 3]. In fact, $\mathcal{O}(g^2a^2)$ flavor violating effects can be completely removed by appropriate choice of the coefficients of the three-, five- and seven-link staples [4]. This results in what is called the fat7 action. Higher order effects can be also suppressed by using iterative fattening of the links together with projection back to the SU(3) group [5, 6]. These actions have better flavor symmetry than the fat7 action, which manifests itself in significantly reduced pion splittings [5, 7]. However, the use of projected fat link actions becomes difficult in dynamical simulations. Therefore, only preliminary studies of finite temperature transitions in QCD are available [8, 9]. So far, the only large scale numerical simulations at finite temperature have been done using so-called stout links [10–12].

Most detailed studies of QCD thermodynamics were done with Asqtad [13, 14] and p4 [15–18] staggered actions, which use unprojected fat links. While the pion spectrum for the Asqtad action has been studied both in quenched [4] and full [19] QCD, little is known about the pion spectrum for the p4 action. Therefore, the aim of the paper is to study the pion masses for the p4 action. We calculate the pion spectrum for three different variants of the p4 action (p4fat3, p4fat7, p4fat7tad) and compare them to the Asqtad and naive staggered actions.

2 Actions

2.1 Staggered action

The Kogut–Susskind action is written as

$$S_{\mathrm{F}} = \sum_x \sum_\mu \eta_\mu(x) \big[\bar\chi(x)\big(U_\mu(x)\chi(x+\mu) - U_\mu^\dagger(x-\mu)\chi(x-\mu)\big)\big] + 2m_q \sum_x \bar\chi(x)\chi(x)\,, \quad (1)$$

[a] e-mail: michaelc@phys.columbia.edu

Table 1. Parameters for the different fermion actions. u_0 is the tadpole-improvement coefficient, $u_0 = \langle \Box \rangle^{1/4}$

Action	c_1	c_{Naik}	c_{knight}	c_3	c_5	c_7	c_{Lepage}
Asqtad	$1/8+3/8+1/8$	$-1/24u_0^2$	0	$1/16u_0^2$	$1/64u_0^4$	$1/384u_0^6$	$-1/16u_0^4$
p4fat3	15/44	0	1/24	3/44	0	0	0
p4fat7	$1/8-1/4$	0	1/24	1/16	1/64	1/384	0
p4fat7tad	$1/8-1/4$	0	$1/24u_0^2$	$1/16u_0^2$	$1/64u_0^4$	$1/384u_0^6$	0
staggered	1	0	0	0	0	0	0

where $\chi(x)$ is a one-component spinor, and $\eta_\mu(x) = (-1)^{x_0+\cdots+x_{\mu-1}}$ are the staggered phases.

By distributing the spinor degrees of freedom over a hypercube, the spin and flavor degrees of freedom are mixed by $O(a^2)$ terms in the action. As outlined by Golterman and Smit [20], there are multiple meson states on the lattice that correspond to distinct physical states. For example, there are 15 different operators, falling into seven distinct irreducible representations that have the quantum numbers of a physical pion.

Because only a U(1) remnant of the continuum chiral symmetry group is preserved, only one of these 15 pions is a true Goldstone boson. The other 14 have non-vanishing masses that are determined by the $O(a^2)$ terms in the action.

2.2 Improved staggered actions

There have been several variants of staggered fermions that seek to improve upon the naive staggered formulation. Two notable examples are the p4 [1] and Naik [21] actions. Both of these actions incorporate an additional three-link term in the fermion derivative. The p4 action includes a bent "knight's move" term, while Asqtad uses the straight Naik term. These two terms are the minimal allowed modifications of the fermion derivative consistent with the symmetries of the staggered formulation.

A general action with both the Naik and the knight's move term is written as

$$\begin{aligned} S_{\text{F}} = {} & 2m_q \sum_x \bar{\chi}(x)\chi(x) + \sum_x \bar{\chi}(x) \sum_\mu \eta_\mu(x) \\ & \times \Big\{ c_{1,0}\big[U_\mu(x)\chi(x+\mu) - U_\mu^\dagger(x-\mu)\chi(x-\mu)\big] \\ & + c_{3,0}\big[U_\mu^{(3,0)}(x)\chi(x+3\mu) - U_\mu^{(3,0)\dagger}(x-3\mu)\chi(x-3\mu)\big] \\ & + c_{1,2} \sum_{\nu\neq\mu} \big[U_{\mu,\nu}^{(1,2)}(x)\chi(x+\mu+2\nu) \\ & - U_{\mu,\nu}^{(1,2)\dagger}(x-\mu-2\nu)\chi(x-\mu-2\nu) \\ & + U_{\mu,\nu}^{(1,-2)}(x)\chi(x+\mu-2\nu) \\ & - U_{\mu,\nu}^{(1,-2)\dagger}(x-\mu+2\nu)\chi(x-\mu-2\nu)\big] \Big\}, \end{aligned} \tag{2}$$

where

$$\begin{aligned} U_\mu^{(3,0)}(x) &= U_\mu(x)U_\mu(x+\mu)U_\mu(x+2\mu)\,, \\ U_{\mu,\nu}^{(1,2)}(x) &= \frac{1}{2}[U_\mu(x)U_\nu(x+\mu)U_\nu(x+\mu+\nu) \\ &\quad + U_\nu(x)U_\nu(x+\nu)U_\mu(x+2\nu)]\,, \\ U_{\mu,\nu}^{(1,-2)}(x) &= \frac{1}{2}\big[U_\mu(x)U_\nu^\dagger(x+\mu-\nu)U_\nu^\dagger(x+\mu-2\nu) \\ &\quad + U_\nu^\dagger(x-\nu)U_\nu^\dagger(x-2\nu)U_\mu(x-2\nu)\big]\,. \end{aligned} \tag{3}$$

For the p4 action, $c_{1,2} = 1/24$, $c_{3,0} = 0$; the Naik action has $c_{1,2} = 0$, $c_{3,0} = -1/48$. In the free-field limit, the Naik action eliminates the $O(a^2)$ errors in the quark propagator. The p4 action is chosen to remove the violations to rotational symmetry in the quark propagator through $O(p^4)$.

2.3 Gauge link smearing

It has been shown that gauge link smearing reduces the amount of flavor symmetry violation in the fermion action [4]. Gauge link smearing involves replacing the one-link term in the fermion action with some linear combination of gauge invariant staples that connect nearest-neighbor sites.

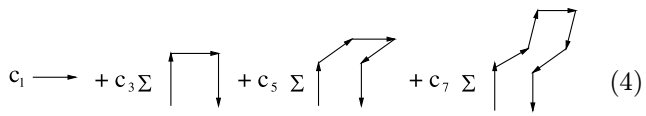

(4)

The p4fat3 action has been used previously in thermodynamic simulations [15]. Only the three-link staple is included for p4fat3. For the so-called fat7 gauge link smearing, the coefficients are chosen to cancel the tree-level violations of flavor symmetry. We use fat7 smearing in the p4fat7 and p4fat7tad actions, employing tadpole improvement in the latter case. The Asqtad action also employs fat7 smearing, including the planar, five-link Lepage term, which eliminates the $O(a^2)$ errors introduced by the smearing procedure [4, 22]. For the p4 actions tested here, the Lepage term has been omitted. A full summary of the smearing parameters can be found in Table 1.

3 Simulation

3.1 Gauge action

We measure the pion spectrum on quenched gauge backgrounds with $\beta = 10/g^2 = 7.40,\ 7.75,\ 8.00$ using a one-loop improved Symanzik action. For each value of β, we

generated 100 configurations. For $\beta = 7.40$, 7.75, we used a volume of $16^3 \times 32$ and separated configurations by 1000 sweeps of the gauge heat bath algorithm. For the finest ensemble, $\beta = 8.00$, we separated configurations by 500 sweeps, on a volume of $24^3 \times 32$. These parameters match those used previously to test the scaling behavior of the Asqtad action [23].

3.2 Sources

Following [24], we calculate the quark propagator for eight different wall sources on each configuration by solving

$$\sum_{x'} (DD^\dagger)(x,x') X^{\vec{A}}(x') = \sum_{2\vec{y}} \delta_{\vec{x},2\vec{y}+\vec{A}} \delta_{x_4,0}\,, \tag{5}$$

$$\chi^{\vec{A}}(x) = \sum_{x'} D^\dagger(x,x') X^{\vec{A}}(x')\,, \tag{6}$$

using the standard conjugate gradient technique. Here the summation over $2\vec{y}$ goes over all the unit cubes at time slice $t = 0$, and $\vec{A}$ labels the eight different corners of a 3D unit cube. We combine the quark propagators that we obtain into meson propagators:

$$M_{\vec{A},\vec{B}} = \sum_x D_{\vec{A}} \bar{\chi}^{\vec{A}}(x) D_{\vec{B}} \chi^{\vec{B}}(x)\,, \tag{7}$$

$$D_{\vec{A}}\chi(x) = \sum_{\delta_1=\pm1} \sum_{\delta_2=\pm1} \sum_{\delta_3=\pm1} \chi(x + \delta_1 A_1 \mathbf{e_1} + \delta_2 A_2 \mathbf{e_2} + \delta_3 A_3 \mathbf{e_3})\,. \tag{8}$$

The 64 different meson operators fall into irreducible representations that can be written as linear combinations of the meson propagators defined above using the symmetric shift operator $D_{\vec{A}}$:

$$M(t) = \sum_{\vec{A}} \phi(\vec{A}) M_{\vec{A},(\vec{A}+\vec{\delta})}\,. \tag{9}$$

$\vec{\delta}$ and $\phi(\vec{A})$ are specified for each irreducible representation. Table 2 lists the details for all the meson representations. In this paper, we consider only those meson operators that correspond to the physical pions in the continuum theory. Henceforth, we shall label the meson states using the conventions set forth in [24], which labels meson states by their transformation properties under the lattice symmetry group ($\mathbf{r}^{\sigma_s\sigma_{123}}$).

Table 2. Staggered pions. $\eta_\mu = (-1)^{A_1+\cdots+A_{\mu-1}}$, $\zeta_\mu = (-1)^{A_{\mu+1}+\cdots+A_4}$, $\epsilon = (-1)^{A_1+\cdots+A_4}$, $\hat{\mathbf{k}} \neq \hat{\mathbf{l}}$

$r^{\sigma_s\sigma_{123}}$	$\phi(\vec{A})$	$\vec{\delta}$
$1++$	1	0
$1+-$	$\eta_4\zeta_4$	0
$3''--$	$\zeta_k\epsilon$	$\hat{\mathbf{k}}$
$3''-+$	$\eta_4\zeta_4\zeta_k\epsilon$	$\hat{\mathbf{k}}$
$3''++$	$\zeta_k\zeta_l\epsilon_{klm}$	$\hat{\mathbf{k}}+\hat{\mathbf{l}}$
$3''+-$	$\eta_4\zeta_4\zeta_k\zeta_l\epsilon_{klm}$	$\hat{\mathbf{k}}+\hat{\mathbf{l}}$
$1--$	$\eta_4\zeta_4\eta_1\eta_2\eta_3$	$\hat{\mathbf{1}}+\hat{\mathbf{2}}+\hat{\mathbf{3}}$

3.3 Measurements

For each set of configurations, we measured the 15 different π propagators for at least three different values of m_q. These values are chosen so that $m_\pi a$ falls into approximately the same range for the different actions. Values of m_π were extracted by fitting to the form

$$M(t) = A(\mathrm{e}^{-m_+ t} + \mathrm{e}^{-m_+(T-t)}) + B(-1)^t(\mathrm{e}^{-m_- t} + \mathrm{e}^{-m_-(T-t)})\,, \tag{10}$$

where m_+ and m_- denote the masses of opposite parity states. By using three masses, we can extrapolate to the $m_q \to 0$ limit.

For $\beta = 8.00$, we use a fitting range of 6–16; for $\beta = 7.75$, a range of 5–16; and for $\beta = 8.00$, we use 4–16 except for staggered fermions, where the larger masses require us to use a fitting range of 3–16 to obtain a good signal.

Tables 3–7 show the values for $m_\pi a$ that we have obtained. While we measure masses for all 15 operators, several of the operators are related by lattice symmetries and fall into degenerate triplets. Our data confirm this expected degeneracy, so we have quoted only one value for each of these triplets by averaging the propagators for each of the degenerate operators. As a result, we are left with seven distinct masses for each set of measurements.

Since neighboring configurations are virtually uncorrelated, errors are calculated by using a single-elimination jackknife. While we only quote statistical errors, there is an additional systematic error associated with varying the fit range. For most of the measurements, we found this effect to be smaller than the quoted statistical error. However, for the coarsest lattices at $\beta = 7.40$, some of the operators have a poorer signal and the resulting masses have systematic errors that are, for some cases, of the same order as the statistical errors.

4 Results

Our data in Tables 3–7 confirm that the π spectrum for the p4 action falls into the same general pattern as shown by previous studies [24]. The state corresponding to the Goldstone pion ($r^{\sigma_s\sigma_{123}} = 1+-$) is clearly lighter than the other pions. We also expect the splittings to be $O(a^2)$, and our data confirm this scaling behavior for the p4 action. Because we use a Symanzik-improved gauge action, the mass splittings are also reduced compared to unimproved gauge actions [25].

In general, we expect the different representations to yield different masses. However, some of the representations are degenerate at $O(a^2)$, differing only at $O(a^4)$ [26]. In particular, we expect the following pairs of representations to be nearly degenerate: $1++$ and $3''--$, $3''-+$

Table 3. Asqtad pion masses

$\mathbf{r}^{\sigma_s\sigma_{123}}$		$\beta = 7.40$			$\beta = 7.75$			$\beta = 8.00$	
$m_q a =$	.02	.03	.04	.02	.03	.04	.01	.02	.03
$1+-$	0.3605(3)	0.4390(3)	0.5047(3)	0.314(1)	0.383(1)	0.440(1)	0.2003(5)	0.2800(5)	0.3409(5)
$1++$	0.644(8)	0.690(4)	0.734(3)	0.399(2)	0.455(2)	0.504(1)	0.247(1)	0.3145(10)	0.3693(8)
$3''--$	0.648(2)	0.698(1)	0.7444(9)	0.401(2)	0.457(1)	0.506(1)	0.2474(7)	0.3142(7)	0.3689(6)
$3''-+$	0.78(1)	0.824(6)	0.863(5)	0.455(3)	0.504(2)	0.548(2)	0.278(2)	0.338(1)	0.3883(10)
$3''++$	0.90(2)	0.93(1)	0.96(1)	0.502(4)	0.543(3)	0.582(3)	0.303(2)	0.358(2)	0.405(1)
$3''+-$	0.802(3)	0.840(2)	0.877(2)	0.456(2)	0.504(1)	0.549(1)	0.2791(8)	0.3379(7)	0.3882(7)
$1--$	0.90(1)	0.935(8)	0.968(6)	0.498(3)	0.541(2)	0.582(2)	0.306(1)	0.3585(8)	0.4049(8)

Table 4. p4fat3 pion masses

$\mathbf{r}^{\sigma_s\sigma_{123}}$		$\beta = 7.40$			$\beta = 7.75$			$\beta = 8.00$	
$m_q a =$	.02	.03	.04	.02	.03	.04	.01	.02	.03
$1+-$	0.3136(2)	0.4395(2)	0.5346(2)	0.2781(6)	0.3893(9)	0.474(1)	0.2469(4)	0.3459(5)	0.4218(5)
$1++$	0.75(3)	0.80(1)	0.861(6)	0.416(3)	0.503(2)	0.576(2)	0.310(2)	0.395(1)	0.4650(8)
$3''--$	0.721(3)	0.792(1)	0.857(1)	0.420(1)	0.504(1)	0.576(1)	0.3094(7)	0.3941(6)	0.4638(6)
$3''-+$	0.94(4)	0.96(2)	1.012(10)	0.495(4)	0.569(3)	0.634(2)	0.348(2)	0.425(1)	0.4905(10)
$3''++$	1.05(8)	1.11(4)	1.14(2)	0.549(6)	0.614(4)	0.673(3)	0.378(3)	0.448(1)	0.510(1)
$3''+-$	0.904(8)	0.966(3)	1.023(3)	0.495(2)	0.568(2)	0.633(2)	0.3481(8)	0.4244(7)	0.4898(7)
$1--$	1.00(3)	1.05(1)	1.112(9)	0.548(4)	0.612(2)	0.672(2)	0.378(1)	0.4477(9)	0.5093(8)

Table 5. p4fat7 pion masses

$\mathbf{r}^{\sigma_s\sigma_{123}}$		$\beta = 7.40$			$\beta = 7.75$			$\beta = 8.00$	
$m_q a =$	.02	.03	.04	.02	.03	.04	.01	.02	.03
$1+-$	0.4205(3)	0.5832(3)	0.7035(3)	0.3216(8)	0.449(1)	0.5467(9)	0.2727(6)	0.3812(6)	0.4651(6)
$1++$	0.681(6)	0.798(3)	0.896(2)	0.395(2)	0.504(2)	0.593(1)	0.302(1)	0.4019(9)	0.4821(7)
$3''--$	0.681(1)	0.8003(9)	0.8999(8)	0.396(2)	0.504(1)	0.593(1)	0.3021(7)	0.4014(7)	0.4815(6)
$3''-+$	0.789(6)	0.895(4)	0.982(3)	0.442(3)	0.539(2)	0.621(2)	0.323(2)	0.416(1)	0.4926(7)
$3''++$	0.90(1)	0.978(6)	1.054(4)	0.484(4)	0.569(3)	0.645(2)	0.341(2)	0.428(1)	0.5019(8)
$3''+-$	0.801(2)	0.901(2)	0.988(1)	0.443(2)	0.539(1)	0.621(1)	0.3233(8)	0.4156(7)	0.4924(7)
$1--$	0.894(6)	0.980(4)	1.057(2)	0.483(2)	0.569(2)	0.645(2)	0.3424(9)	0.4283(8)	0.5019(7)

Table 6. p4fat7tad pion masses

$\mathbf{r}^{\sigma_s\sigma_{123}}$		$\beta = 7.40$			$\beta = 7.75$			$\beta = 8.00$	
$m_q a =$	.02	.03	.04	.02	.03	.04	.01	.02	.03
$1+-$	0.4227(3)	0.5139(3)	0.5900(3)	0.449(1)	0.5467(9)	0.6293(9)	0.2161(6)	0.3015(6)	0.3669(6)
$1++$	0.643(4)	0.708(3)	0.766(2)	0.504(2)	0.593(1)	0.671(1)	0.250(2)	0.326(1)	0.3870(10)
$3''--$	0.6476(10)	0.7124(9)	0.7708(8)	0.504(1)	0.593(1)	0.670(1)	0.2518(9)	0.3263(7)	0.3866(7)
$3''-+$	0.762(5)	0.816(4)	0.867(3)	0.539(2)	0.621(2)	0.695(1)	0.276(2)	0.345(2)	0.402(1)
$3''++$	0.873(10)	0.915(6)	0.956(5)	0.569(3)	0.645(2)	0.715(2)	0.300(3)	0.361(2)	0.414(1)
$3''+-$	0.775(2)	0.828(2)	0.877(1)	0.539(1)	0.621(1)	0.695(1)	0.279(1)	0.3452(8)	0.4014(7)
$1--$	0.869(7)	0.915(4)	0.957(3)	0.569(2)	0.645(2)	0.715(1)	0.302(1)	0.3622(8)	0.4147(8)

and $3''+-$, and $3''++$ and $1--$. This approximate degeneracy is evident for the p4 action. Our precision is not enough to discern the expected pattern of $O(a^4)$ splittings.

Using the data collected in Tables 3–7, we extrapolate each of the 15 different pions to the chiral limit ($m_q \to 0$). These fits were done using the expected chiral form:

$$m_\pi^2(m_q) = m_\pi^2(m_q = 0) + B m_q \,. \tag{11}$$

Figure 1 shows the result of a typical chiral fit for each of the seven distinct representations. Tables 8–10 give the

Table 7. Naive staggered pion masses

$\mathbf{r}^{\sigma_s\sigma_{123}}$	$\beta = 7.40$				$\beta = 7.75$			
$m_q a =$	.01	.02	.03	.04	.01	.02	.03	.04
$1+-$	0.2738(2)	0.3834(2)	0.4655(2)	0.5332(2)	0.2769(4)	0.3861(4)	0.4676(4)	0.5351(4)
$1++$	0.93(4)	0.98(2)	1.02(1)	1.063(10)	0.540(8)	0.617(4)	0.687(3)	0.749(2)
$3''--$	0.941(5)	0.997(4)	1.045(3)	1.090(2)	0.539(2)	0.620(2)	0.689(1)	0.750(1)
$3''-+$	1.2(1)	1.23(3)	1.26(3)	1.29(2)	0.631(8)	0.698(5)	0.762(4)	0.820(3)
$3''++$	1.18(6)	1.25(3)	1.31(2)	1.36(2)	0.67(1)	0.731(6)	0.793(5)	0.849(4)
$3''+-$	1.13(1)	1.171(7)	1.218(5)	1.264(4)	0.618(4)	0.690(2)	0.755(2)	0.815(2)
$1--$	1.16(3)	1.25(2)	1.31(1)	1.36(1)	0.664(7)	0.732(4)	0.795(3)	0.851(3)

$\mathbf{r}^{\sigma_s\sigma_{123}}$	$\beta = 8.00$		
$m_q a =$	.01	.02	.03
$1+-$	0.2580(3)	0.3604(3)	0.4379(3)
$1++$	0.381(2)	0.467(1)	0.5393(8)
$3''--$	0.3805(7)	0.4660(6)	0.5379(6)
$3''-+$	0.425(2)	0.502(1)	0.572(1)
$3''++$	0.449(3)	0.523(2)	0.590(1)
$3''+-$	0.4215(10)	0.5008(8)	0.5698(7)
$1--$	0.447(1)	0.523(1)	0.5889(9)

Table 8. m_π extrapolated to $m_q = 0$ for $\beta = 7.40$

$\mathbf{r}^{\sigma_s\sigma_{123}}$	Asqtad	p4fat3	p4fat7	p4fat7tad	Staggered
$1+-$	0.072(1)	0.0675(7)	0.1317(9)	0.096(1)	0.0723(4)
$1++$	0.54(1)	0.68(3)	0.545(9)	0.490(9)	0.88(4)
$3''--$	0.534(3)	0.642(3)	0.540(2)	0.49(2)	0.890(6)
$3''-+$	0.69(2)	0.88(3)	0.677(9)	0.639(8)	1.18(6)
$3''++$	0.84(3)	1.02(10)	0.81(2)	0.78(2)	1.13(5)
$3''+-$	0.719(6)	0.841(10)	0.691(4)	0.658(3)	1.07(1)
$1--$	0.83(2)	0.93(3)	0.802(9)	0.77(1)	1.11(3)

Table 9. m_π extrapolated to $m_q = 0$ for $\beta = 7.75$

$\mathbf{r}^{\sigma_s\sigma_{123}}$	Asqtad	p4fat3	p4fat7	p4fat7tad	Staggered
$1+-$	0.064(3)	0.061(2)	0.075(3)	0.086(4)	0.08(1)
$1++$	0.253(4)	0.307(5)	0.240(4)	0.239(3)	0.449(9)
$3''--$	0.257(2)	0.314(2)	0.244(2)	0.243(2)	0.449(2)
$3''-+$	0.339(5)	0.408(6)	0.317(4)	0.314(4)	0.552(9)
$3''++$	0.407(7)	0.474(9)	0.377(5)	0.370(5)	0.59(1)
$3''+-$	0.338(3)	0.409(3)	0.319(2)	0.315(3)	0.537(5)
$1--$	0.397(4)	0.473(6)	0.377(3)	0.370(3)	0.590(8)

Table 10. m_π extrapolated to $m_q = 0$ for $\beta = 8.00$

$\mathbf{r}^{\sigma_s\sigma_{123}}$	Asqtad	p4fat3	p4fat7	p4fat7tad	Staggered
$1+-$	0.046(2)	0.050(2)	0.058(3)	0.052(2)	0.063(1)
$1++$	0.152(3)	0.191(3)	0.142(3)	0.138(4)	0.268(4)
$3''--$	0.154(1)	0.190(1)	0.145(1)	0.143(1)	0.269(1)
$3''-+$	0.201(3)	0.248(3)	0.186(3)	0.185(3)	0.326(4)
$3''++$	0.237(4)	0.290(4)	0.219(3)	0.222(4)	0.357(5)
$3''+-$	0.204(1)	0.248(1)	0.188(1)	0.189(1)	0.323(2)
$1--$	0.242(2)	0.290(2)	0.223(1)	0.226(2)	0.356(2)

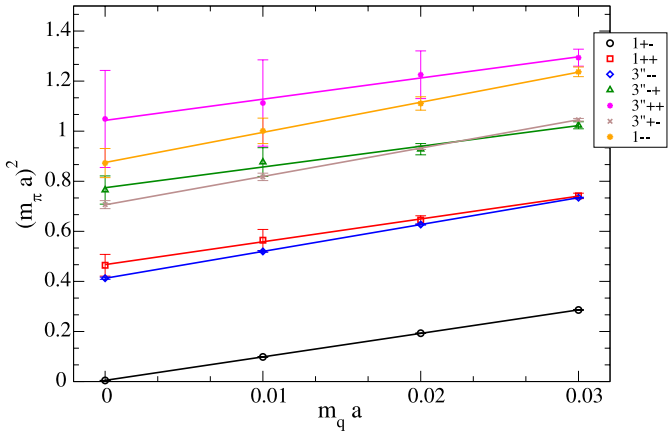

Fig. 1. Chiral extrapolation of m_π^2 for p4fat3 action, $\beta = 7.40$ on a $16^3 \times 32$ volume

full result of these extrapolations. In the continuum limit, we expect the Goldstone pion to have a vanishing mass as $m_q \to 0$. In our case, m_π does not exactly vanish at $m_q = 0$ due to finite volume effects.

Figures 2–4 show the chiral extrapolated values of m_π. The p4fat3 action, which uses three-link smearing, is a significant improvement over the naive staggered action. As expected, the three actions with $\mathcal{O}(g^2a^2)$ improvement (Asqtad, p4fat7, p4fat7tad) show the best flavor symmetry characteristics and give similar results. For $\beta = 7.40$, p4fat7 and Asqtad agree to within statistical errors, while p4fat7tad is very slightly better. For $\beta = 7.75$ and $\beta = 8.00$, the p4 actions are slightly better than Asqtad. This difference is likely due to the inclusion of the Lepage term in the Asqtad action, which does not help suppress flavor symmetry breaking, but which does cancel $\mathcal{O}(a^2)$ effects [22]. Tadpole improvement seems to have little effect on the p4 action – p4fat7 and p4fat7tad agree to within errors. Similar observations have been made with respect to the Naik action [4]. Figure 5 shows the mass splitting as a function

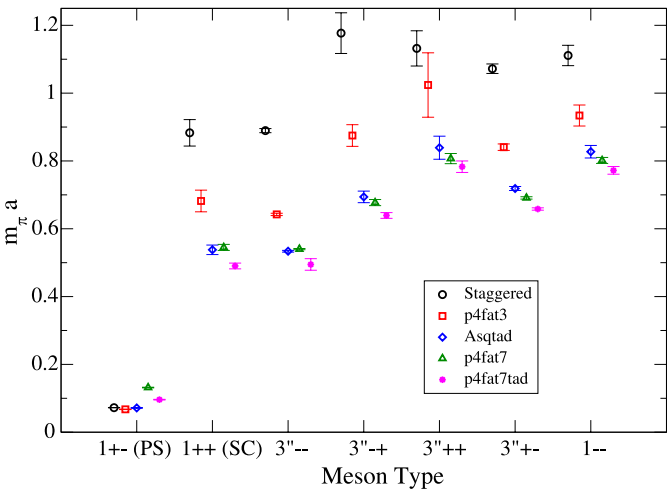

Fig. 2. Flavor symmetry breaking of m_π in the chiral limit for $\beta = 7.40$ on a $16^3 \times 32$ volume

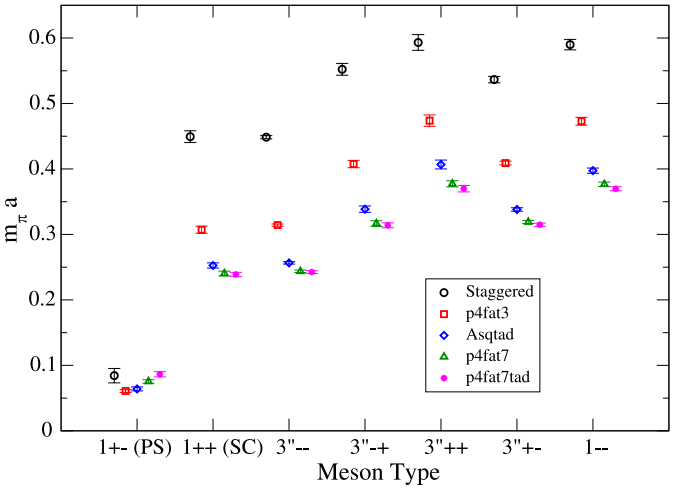

Fig. 3. Flavor symmetry breaking of m_π in the chiral limit for $\beta = 7.75$ on a $16^3 \times 32$ volume

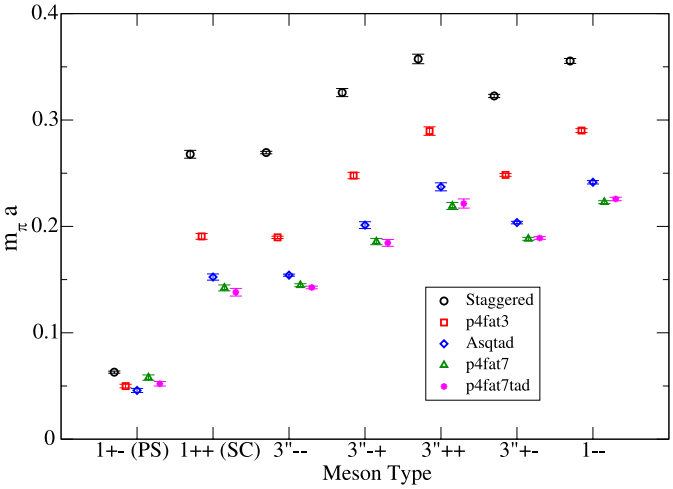

Fig. 4. Flavor symmetry breaking of m_π in the chiral limit for $\beta = 8.00$ on a $24^3 \times 32$ volume

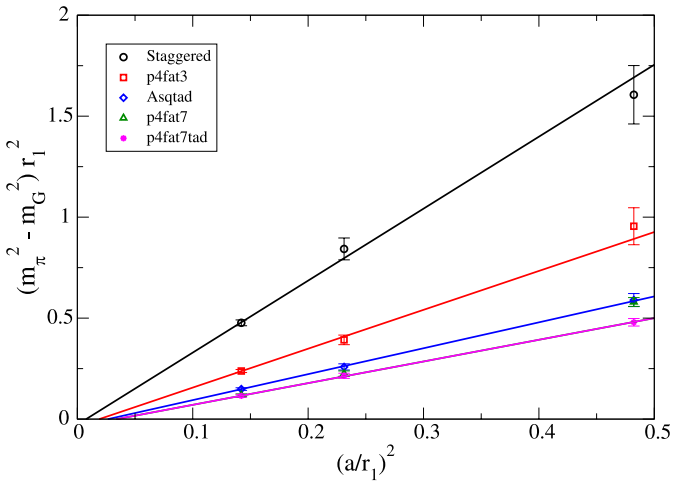

Fig. 5. Pion mass splittings for chirally extrapolated values of m_π. m_π corresponds to $r^{\sigma_s \sigma_{123}} = 1++$, while m_G is the mass of the Goldstone pion

of a^2. As expected, the quantity $m_\pi^2 - m_G^2$ vanishes linearly with a^2 for each of the actions.

5 Conclusions

We have performed a detailed study of flavor symmetry violation in the π spectrum for three different variants of the p4 action.

As expected, $\mathcal{O}(a^2)$ flavor symmetry violations are most severe for the coarsest lattices. The flavor symmetry properties of the fat7-improved p4 actions match those of Asqtad very closely. While the p4fat3 action is poorer in this respect than its fat7 cousins, it is markedly better than unimproved staggered ones. As expected, gauge link fattening is the most important factor in determining flavor symmetry breaking. Furthermore, we see that tadpole improvement has very little effect on the pattern of flavor symmetry breaking for the p4 action, as well.

Acknowledgements. This work has been supported in part by contracts DE-AC02-98CH1-886 and DE-FG02-92ER40699 with the U.S. Department of Energy,

We thank RIKEN, Brookhaven National Laboratory and the U.S. Department of Energy for providing the facilities essential for the completion of this work. The numerical computations were done on the QCDOC computers, located at Columbia University and Brookhaven National Lab.

References

1. U.M. Heller, F. Karsch, B. Sturm, Phys. Rev. D **60**, 114502 (1999) [hep-lat/9901010]
2. T. Blum et al., Phys. Rev. D **55**, 1133 (1997) [hep-lat/9609036]
3. J.F. Lagae, D.K. Sinclair, Phys. Rev. D **59**, 014511 (1999) [hep-lat/9806014]
4. MILC, K. Orginos, D. Toussaint, R.L. Sugar, Phys. Rev. D **60**, 054503 (1999) [hep-lat/9903032]
5. A. Hasenfratz, F. Knechtli, Phys. Rev. D **64**, 034504 (2001) [hep-lat/0103029]
6. HPQCD, E. Follana et al., hep-lat/0610092 (2006)
7. T. Bae, J. Kim, W. Lee, S.R. Sharpe, hep-lat/0610056 (2006)
8. A. Hasenfratz, F. Knechtli, hep-lat/0105022 (2001)
9. P. Petreczky, J. Phys. G **30**, S1259 (2004)
10. Y. Aoki, G. Endrodi, Z. Fodor, S.D. Katz, K.K. Szabo, Nature **443**, 675 (2006) [hep-lat/0611014]
11. Y. Aoki, Z. Fodor, S.D. Katz, K.K. Szabo, Phys. Lett. B **643**, 46 (2006) [hep-lat/0609068]
12. Y. Aoki, Z. Fodor, S.D. Katz, K.K. Szabo, JHEP **01**, 089 (2006) [hep-lat/0510084]
13. MILC, C. Bernard et al., Phys. Rev. D **71**, 034504 (2005) [hep-lat/0405029]
14. C. Bernard et al., hep-lat/0611031 (2006)
15. F. Karsch, E. Laermann, A. Peikert, Nucl. Phys. B **605**, 579 (2001) [hep-lat/0012023]
16. F. Karsch, E. Laermann, A. Peikert, Phys. Lett. B **478**, 447 (2000) [hep-lat/0002003]
17. M. Cheng et al., Phys. Rev. D **75**, 034506 (2007) [hep-lat/0612001]
18. M. Cheng et al., Phys. Rev. D **74**, 054507 (2006) [hep-lat/0608013]
19. C. Aubin et al., Phys. Rev. D **70**, 094505 (2004) [hep-lat/0402030]
20. M.F.L. Golterman, Nucl. Phys. B **273**, 663 (1986)
21. S. Naik, Nucl. Phys. B **316**, 238 (1989)
22. G.P. Lepage, Phys. Rev. D **59**, 074502 (1999) [hep-lat/9809157]
23. MILC, C.W. Bernard et al., Phys. Rev. D **61**, 111502 (2000) [hep-lat/9912018]
24. N. Ishizuka, M. Fukugita, H. Mino, M. Okawa, A. Ukawa, Nucl. Phys. B **411**, 875 (1994)
25. T.A. DeGrand, A. Hasenfratz, T.G. Kovacs, Phys. Rev. D **67**, 054501 (2003) [hep-lat/0211006]
26. W.-J. Lee, S.R. Sharpe, Phys. Rev. D **60**, 114503 (1999) [hep-lat/9905023]